NASA/TM-2003-212149

CFD Variability for a Civil Transport Aircraft Near Buffet-Onset Conditions

Christopher L. Rumsey, Joseph H. Morrison, and Robert T. Biedron
Langley Research Center, Hampton, Virginia

February 2003

The NASA STI Program Office ... in Profile

Since its founding, NASA has been dedicated to the advancement of aeronautics and space science. The NASA Scientific and Technical Information (STI) Program Office plays a key part in helping NASA maintain this important role.

The NASA STI Program Office is operated by Langley Research Center, the lead center for NASA's scientific and technical information. The NASA STI Program Office provides access to the NASA STI Database, the largest collection of aeronautical and space science STI in the world. The Program Office is also NASA's institutional mechanism for disseminating the results of its research and development activities. These results are published by NASA in the NASA STI Report Series, which includes the following report types:

- TECHNICAL PUBLICATION. Reports of completed research or a major significant phase of research that present the results of NASA programs and include extensive data or theoretical analysis. Includes compilations of significant scientific and technical data and information deemed to be of continuing reference value. NASA counterpart of peer-reviewed formal professional papers, but having less stringent limitations on manuscript length and extent of graphic presentations.

- TECHNICAL MEMORANDUM. Scientific and technical findings that are preliminary or of specialized interest, e.g., quick release reports, working papers, and bibliographies that contain minimal annotation. Does not contain extensive analysis.

- CONTRACTOR REPORT. Scientific and technical findings by NASA-sponsored contractors and grantees.

- CONFERENCE PUBLICATION. Collected papers from scientific and technical conferences, symposia, seminars, or other meetings sponsored or co-sponsored by NASA.

- SPECIAL PUBLICATION. Scientific, technical, or historical information from NASA programs, projects, and missions, often concerned with subjects having substantial public interest.

- TECHNICAL TRANSLATION. English-language translations of foreign scientific and technical material pertinent to NASA's mission.

Specialized services that complement the STI Program Office's diverse offerings include creating custom thesauri, building customized databases, organizing and publishing research results ... even providing videos.

For more information about the NASA STI Program Office, see the following:

- Access the NASA STI Program Home Page at ***http://www.sti.nasa.gov***

- E-mail your question via the Internet to help@sti.nasa.gov

- Fax your question to the NASA STI Help Desk at (301) 621-0134

- Phone the NASA STI Help Desk at (301) 621-0390

- Write to:
  NASA STI Help Desk
  NASA Center for AeroSpace Information
  7121 Standard Drive
  Hanover, MD 21076-1320

NASA/TM-2003-212149

CFD Variability for a Civil Transport Aircraft Near Buffet-Onset Conditions

Christopher L. Rumsey, Joseph H. Morrison, and Robert T. Biedron
Langley Research Center, Hampton, Virginia

National Aeronautics and
Space Administration

Langley Research Center
Hampton, Virginia 23681-2199

February 2003

Available from:

NASA Center for AeroSpace Information (CASI)
7121 Standard Drive
Hanover, MD 21076-1320
(301) 621-0390

National Technical Information Service (NTIS)
5285 Port Royal Road
Springfield, VA 22161-2171
(703) 605-6000

Contents

ABSTRACT **iv**

1 INTRODUCTION **1**

2 METHODOLOGY **2**

2.1 Description of CFD Codes 2

2.2 Description of Grid 2

2.3 Summary of Computations Performed 4

3 RESULTS **8**

4 CONCLUDING REMARKS **16**

ACKNOWLEDGMENTS **16**

ABSTRACT

A CFD sensitivity analysis is conducted for an aircraft at several conditions, including flow with substantial separation (buffet onset). The sensitivity is studied using two different Navier-Stokes computer codes, three different turbulence models, and two different grid treatments of the wing trailing edge. This effort is a follow-on to an earlier study of CFD variation over a different aircraft in buffet onset conditions. Similar to the earlier study, the turbulence model is found to have the largest effect, with a variation of 3.8% in lift at the buffet onset angle of attack. Drag and moment variation are 2.9% and 23.6%, respectively. The variations due to code and trailing edge cap grid are smaller than that due to turbulence model. Overall, the combined approximate error band in CFD due to code, turbulence model, and trailing edge treatment at the buffet onset angle of attack are: 4% in lift, 3% in drag, and 31% in moment. The CFD results show similar trends to flight test data, but also exhibit a lift curve break not seen in the data.

1 INTRODUCTION

CFD codes are now run routinely for complex aerodynamic configurations, both for the purpose of aircraft design as well as to assess and improve the capability of CFD to predict certain classes of flows. While many engineers have begun to trust CFD results for mostly attached flows (such as aircraft at cruise conditions), the same cannot be said for separated or unsteady flows. Some of the fault for this may be that current turbulence models or any Reynolds-averaged Navier-Stokes (RANS) models are unable to handle some of the complex, inherently-unsteady physics involved. But it is also more difficult to obtain reliable experimental data at these conditions, so some of the fault may be attributed to difficulty in using CFD to model precisely the same problem as experiment.

Recently, Rumsey et al.[1] examined the CFD sensitivity for a civil transport near buffet onset. Grid, code, spatial differencing method, aeroelastic shape, and turbulence model were varied. In summary, given a grid of sufficient density for a given aeroelastic wing shape, the combined approximate error band in CFD at conditions near buffet onset due to code, spatial differencing method, and turbulence model were: 6% in lift, 7% in drag, and 16% in moment. The biggest two contributors to this uncertainty were turbulence model and code.

Using the knowledge gleaned from the earlier study, another aircraft configuration was investigated. This paper details some of our experiences computing this new flow in flight conditions near buffet onset. This time, due to the fact that they were the largest influences before, turbulence model and computer code were still varied. Additionally, because of this aircraft's blunt wing trailing edge, the effect of changing the modeling of the trailing edge shape in the CFD grid was also explored. In the current study, comparisons were made with flight test data only. It is not believed to be appropriate to compare the current CFD results with wind tunnel data, because the CFD cases used the flight geometry (not the wind tunnel geometry, which employed a different fuselage shape).

The complete grid system in the current study was designed using many of the "lessons learned" in the previous study. Based on the grid sensitivity study from Ref. [1], the current grid is believed to be fine enough to adequately capture the forces and moments to within a significantly lower error than the errors due to code or turbulence model.

In the following section, the methodology is presented, including a brief description of the CFD codes, the grid system, and a summary of the computations performed. Following the methodology, results and concluding remarks are given.

2 METHODOLOGY

2.1 Description of CFD Codes

Two different CFD codes were employed in this study: CFL3D [2] and OVERFLOW [3]. Both codes were developed at NASA. Both are multi-zone codes in wide use in U.S. industry. Both can use overset grids, and both employ local time step scaling, grid sequencing, and multigrid to accelerate convergence to steady state. Time-accurate modes are also available for both codes, and both can employ low-Mach number preconditioning for accuracy in computing low-speed steady-state flows.

CFL3D is a finite volume method. It uses third-order upwind-biased spatial differencing on the convective and pressure terms, and second-order differencing on the viscous terms; it is globally second-order spatially accurate. The flux difference-splitting (FDS) method of Roe is employed to obtain fluxes at the cell faces. It is advanced in time with an implicit three-factor approximate factorization method.

OVERFLOW is a finite difference method. It can use either second-order central differencing or third-order FDS. Left-hand side options include a diagonalized (scalar pentadiagonal) scheme and an LU-SGS scheme. First-order implicit time advancement is used. For this study, both CFL3D and OVERFLOW employed the PEGSUS [4] software to obtain overset interpolants for the regions of overlapping grid.

Three turbulence models were used for the current study. These were: Spalart-Allmaras (SA) [5], Menter's shear stress transport (SST) k-ω [6], and an explicit algebraic stress model (EASM) in k-ω form [7]. It should be noted that OVERFLOW employs an unpublished variation of the SA model (see Ref. [1]). However, at high Reynolds numbers like that used in the current study, the effect is almost negligible.

2.2 Description of Grid

The baseline overset grid system for this configuration was composed of 31 zones, with a total of over 11.8 million grid points. The grid used the flight geometry (as opposed to the wind tunnel model geometry), and used different flight aeroelastic wing shapes for each of three different angles of attack.

The general rules from Ref. [1] for grid point spacings, grid stretching, trailing-edge closure, and wake-cut placement were followed for the current grid. However, because the current configuration had flap hinge fairings and a winglet, the resulting total number of grid points was considerably greater than the baseline grid from the earlier reference. The minimum spacings at solid surfaces was such that the average minimum y^+ level was approximately 1.4. The far field grid extent was at least 50 mean aerodynamic chords. Two views showing the surface grid are given in Figs. 1 and 2. Fig. 1 shows an overall view of the fuselage, wing, winglet, pylon, and nacelle. Fig. 2 shows some details on the lower surface of the wing, including the grid spacing on the wing itself and the C-grid topology around the three flap hinge fairings. Fig. 3 renders the grid as a smooth surface to show a clearer view of the geometry of the flap hinge fairings as well as the nacelle.

A few runs were also performed for which the wing trailing edge geometry was modeled realistically (using a cap grid), rather than simply closing off the trailing edge with one grid point (as was done for the baseline grid). This latter method, described more fully in Ref. [1],

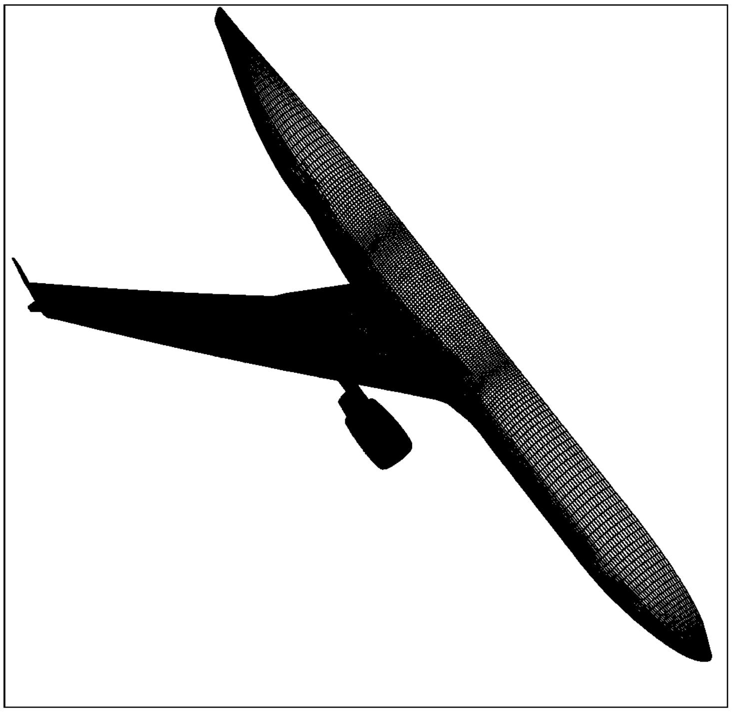

Figure 1: Overall view of aircraft configuration.

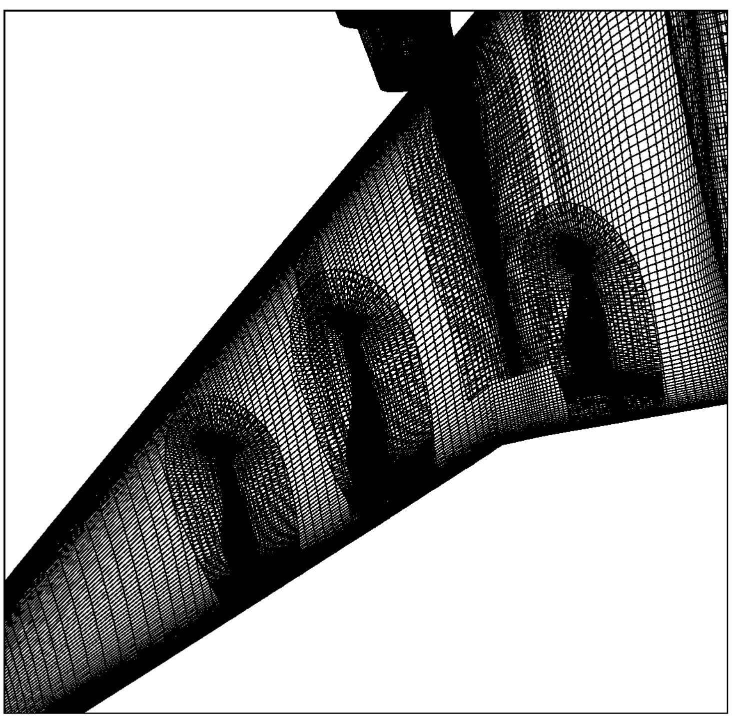

Figure 2: View of grid over lower surface of wing, including flap hinge fairings.

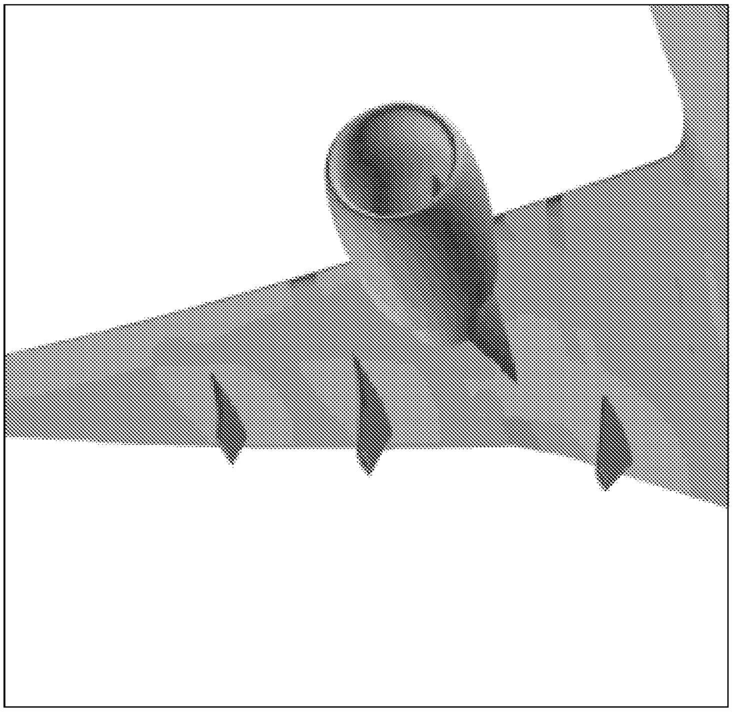

Figure 3: Smooth surface view of lower surface of wing, including flap hinge fairings and nacelle.

has been found to yield reasonable force and moment predictions for many configurations. However, the current configuration possesses a very blunt trailing edge, which may have more of an influence on the results if it is not faithfully modeled.

Views of the trailing edge for the baseline as well as the capped trailing edge are shown in Figs. 4, 5, 6, and 7. For the capped grid, the blunt base of the trailing edge at each spanwise station was modeled with 41 grid points. From Figs. 5 and 7, it should be noted that, although the cap grid models the blunt trailing edge shape, it also possesses significantly larger wake spreading than the baseline grid. This spreading may introduce excessive numerical dissipation in the near wake region, and also may introduce large overset interpolation errors at the interface between the two grid zones because of the large difference in grid spacings. On the other hand, sometimes faithfully modeling the blunt trailing edge and including fine wake resolution results in an unsteady solution (because of alternating shed vortices). While this situation is more physically realistic, it is also extremely costly because the CFD codes must be run time-accurately. We did not pursue this avenue of exploration for the current study.

2.3 Summary of Computations Performed

A summary of the computations performed for the current study is given in Table 1. Half the runs were made using OVERFLOW and half with CFL3D. OVERFLOW only used the SA turbulence model, whereas CFL3D employed the SA model as well as SST and EASM. The effect of the trailing edge capped grid was tested using OVERFLOW. The aeroelastic shape appropriate to each angle of attack was employed for $\alpha = 3.9°$, $4.3°$, and $5.2°$. However, at angles of attack higher than $\alpha = 5.2°$, new aeroelastically-correct grids were not created. In the previous study (Ref. [1]), at angles of attack beyond buffet onset the aeroelastic shape did not change as much as it did at lower angles of attack, because wing loading did not increase as much with α. The same trend was found to hold in the present case. Therefore, use of the grid created for $\alpha = 5.2°$ is believed to be a reasonable approximation at the higher angles.

All cases were run at a Mach number of 0.82 and a Reynolds number of 55 million (based on mean aerodynamic chord). All runs were performed fully turbulent. Due to time and budget constraints, a grid sensitivity study was not performed for this configuration. Performing such a study would have required creating both finer and coarser grid systems. It is believed that taking every other grid point from the existing grid size of 11.8 million points would yield a grid too coarse to provide meaningful results (i.e., it lies outside of the asymptotic range in which grid refinement or coarsening yields results that follow the spatial order property of the numerical scheme). Based on the grid sensitivity study performed in Ref. [1], the current grid size is believed to be fine enough to adequately capture the forces and moments to within a significantly lower error than the errors due to code or turbulence model.

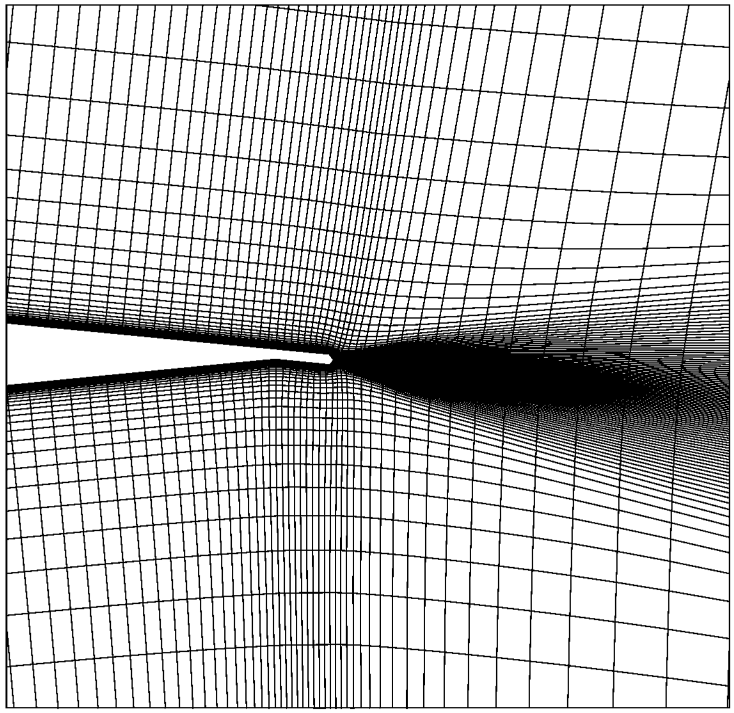

Figure 4: View of wing trailing edge, baseline grid.

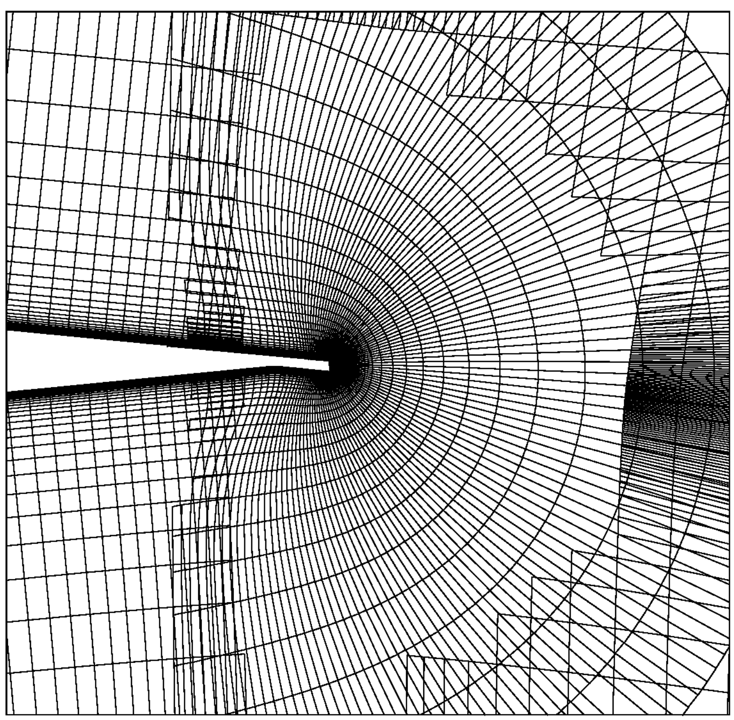

Figure 5: View of wing trailing edge, capped-trailing-edge grid.

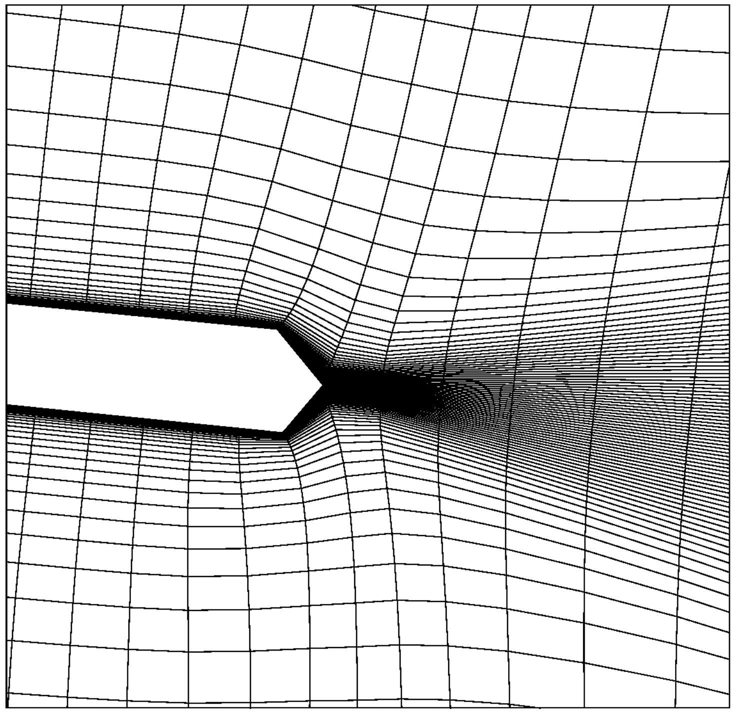

Figure 6: Close-up view of wing trailing edge, baseline grid.

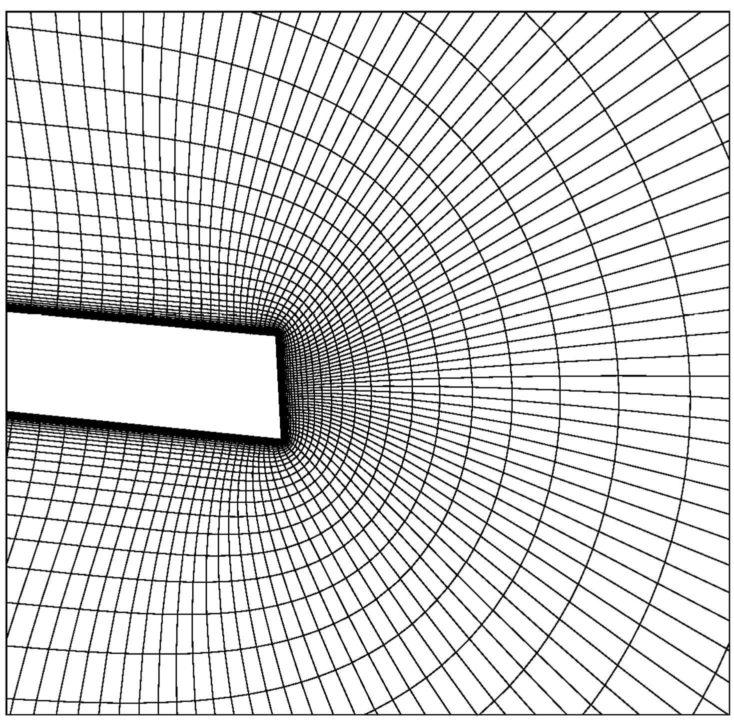

Figure 7: Close-up view of wing trailing edge, capped-trailing-edge grid.

3 RESULTS

Fig. 8 gives a summary plot of the computed lift curve compared to flight test data from Clark and Pelkman [8]. The flight test data was corrected to a tail-off condition. The lift coefficient at which buffet onset occurs in the flight test (acceleration of ± 0.10g at center of gravity) is shown.

Overall, the CFD results as a whole track the flight test data relatively well through buffet onset. However, there clearly are discrepancies: the lift is too high at the lower angles and too low at the higher angles. Thus, the CFD is indicating a break in the lift curve slope somewhere between $\alpha = 4.3°$ and $5.2°$ that is not exhibited in the flight data. However, the reader should be cautioned that many of the particulars of the flight data's genesis are not fully understood (see also the discussion on this topic in Ref. [1]). Therefore, the comparison should be viewed in a qualitative light only. Drag and moment coefficients are plotted in Figs. 9 and 10, respectively. No flight data was available to compare with these quantities.

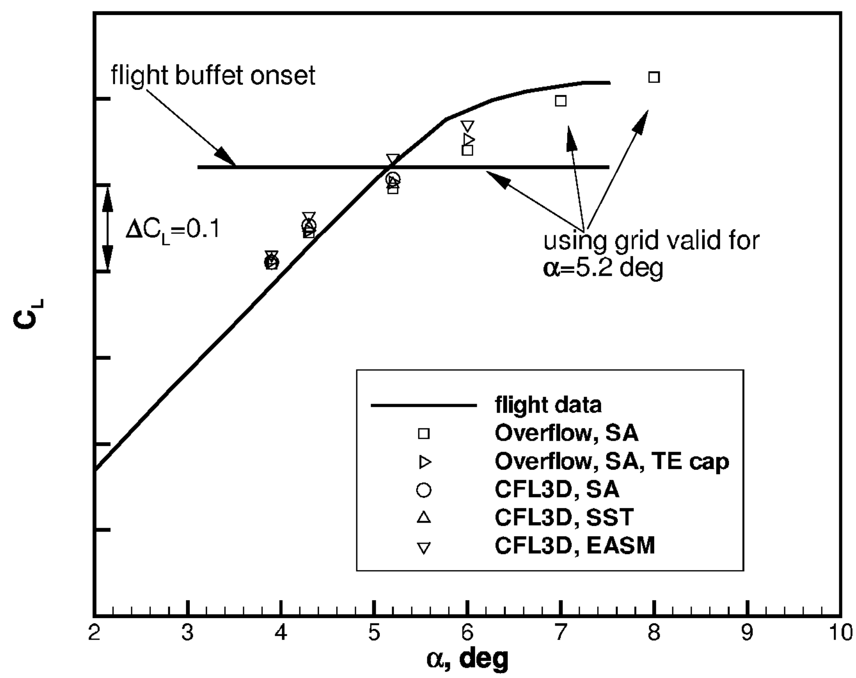

Figure 8: Computed lift coefficients compared with flight test data (corrected to tail-off condition).

The variations in the CFD results are summarized in Tables 2, 3, and 4, for effects of code, turbulence model, and cap grid, respectively. The lift and drag coefficient differences at the three angles of attack of $\alpha = 3.9°$, $4.3°$, and $5.2°$ are represented graphically in Fig. 11. In general, the higher the angle of attack, the larger the variation. The largest of the three individual effects is the effect of turbulence model. The variation due to the cap grid is generally

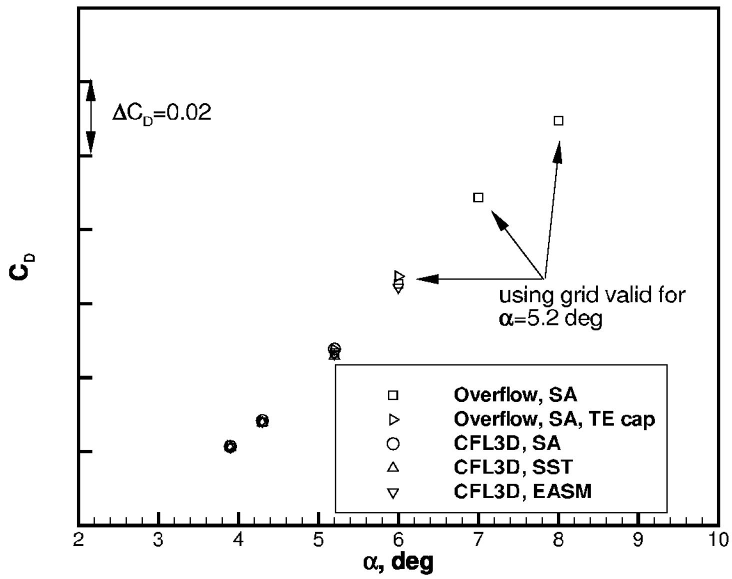

Figure 9: Computed drag coefficients.

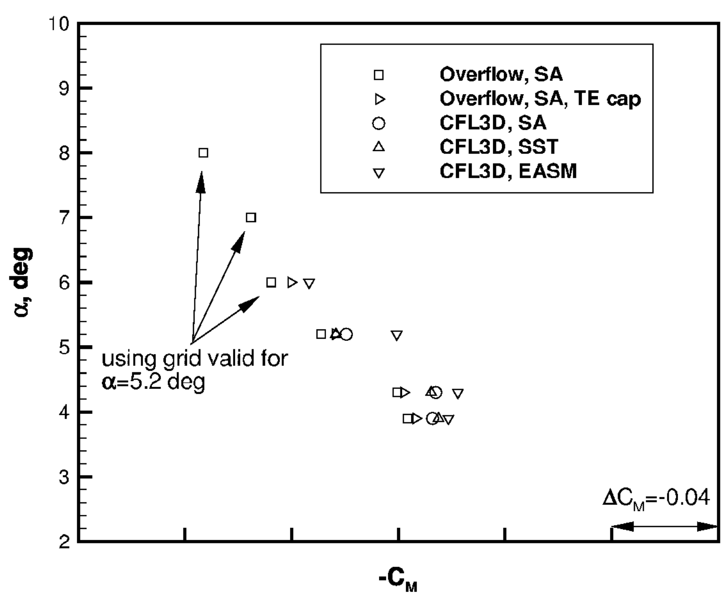

Figure 10: Computed moment coefficients.

lower than that due to code.

This figure can be compared to Fig. 18 in Ref. [1]. For that earlier configuration, similar trends were seen between variations due to code and turbulence model: for example, at buffet onset the variation in lift was about 3% due to turbulence model and about 2% due to code. For the current configuration at buffet onset ($\alpha = 5.2°$), the numbers are 3.8% and 1.3%.

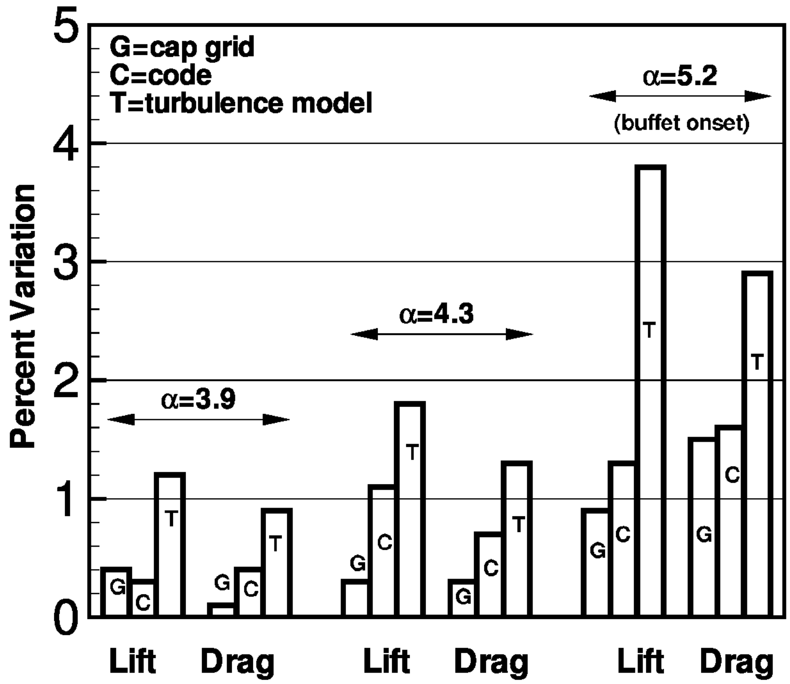

Figure 11: Graphical summary of CFD variations.

The progression of upper surface streamline patterns for three successive angles of attack of $\alpha = 3.9°$, $4.3°$, and $5.2°$ are shown (for results using the SA model in CFL3D) in Figs. 12, 13, and 14, respectively. At the lowest angle of attack, there is a small region of shock-induced separation. This region grows as the angle of attack is increased. At the buffet-onset angle of $\alpha = 5.2°$, a significant portion of the wing upper surface is separated.

Streamlines that demonstrate the effect of turbulence model on the wing upper surface flowfield at $\alpha = 5.2°$ are shown in Figs. 14, 15 and 16. These solutions are given by the SA, SST, and EASM turbulence models, respectively. The SST model yields the lowest lift and EASM the highest, giving a difference of 3.8%. (The EASM yields the smallest of the three separated regions, due to its further-aft shock location.) The difference in separated-region sizes between the turbulence models also has a very large impact on the computed pitching moment (23.6%).

The computed streamlines at $\alpha = 5.2°$ can be compared with the separation pattern from the flight test, shown schematically in Fig. 17. As was also the case in Clark and Pelkman [8], CFD generally predicts the onset of separation (i.e., the shock location) further forward than experiment. Among the three turbulence models used in this study, EASM predicts the furthest aft shock location and thus gives the best qualitative agreement with the flight test.

Wing upper surface pressure coefficients are shown at nine span stations in Fig. 18, comparing SA results using CFL3D and OVERFLOW. No flight data was available for comparison. Results are very close except at the span stations between 2y/B = 0.7 and 0.9 inclusive, where CFL3D predicts the shock location to be further forward than OVERFLOW by as much as 5% chord. Also, the C_p levels tend to be lower in the separated region behind the shock for CFL3D.

Taking the largest differences between *any* of the CFD runs at the buffet onset condition of $\alpha = 5.2°$, the combined approximate error band in CFD due to code, turbulence model, and trailing edge treatment were: 4% in lift, 3% in drag, and 31% in moment. The variation in moment is so large because it is the most sensitive of the three quantities to differences in surface pressures. At buffet onset in particular, the separated region on the wing is quite extensive for this configuration, and small differences in the region's shape have a profound effect on the integrated moment.

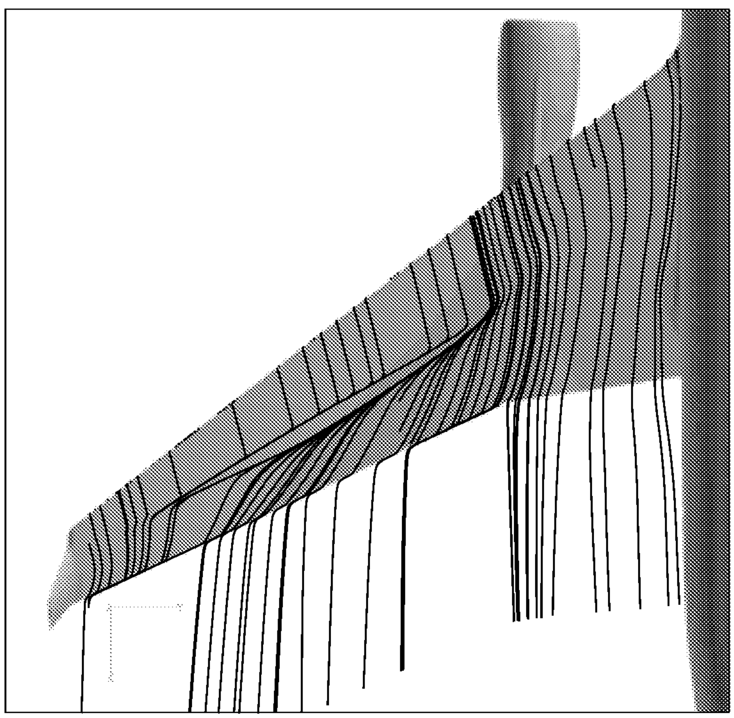

Figure 12: Wing upper surface streamlines, $\alpha = 3.9°$, CFL3D, SA.

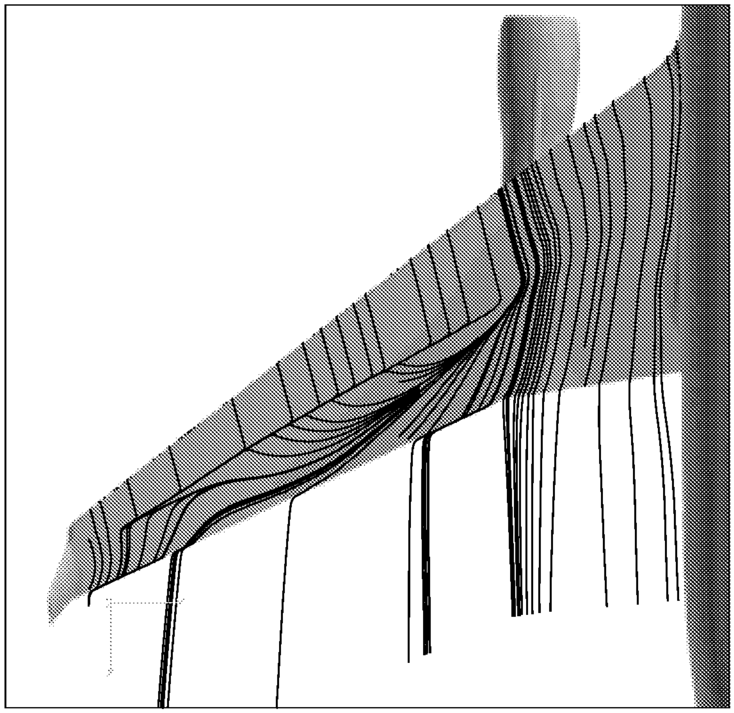

Figure 13: Wing upper surface streamlines, $\alpha = 4.3°$, CFL3D, SA.

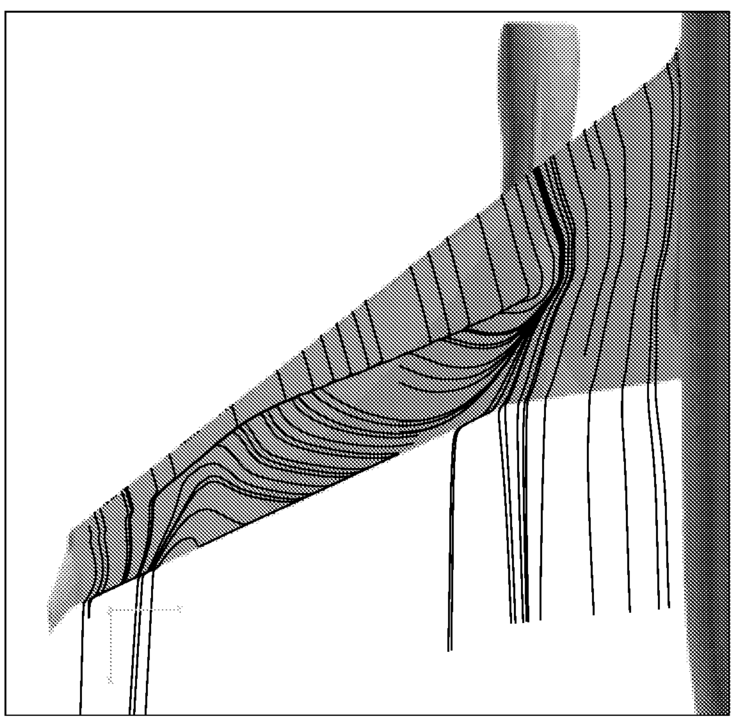

Figure 14: Wing upper surface streamlines, $\alpha = 5.2°$, CFL3D, SA.

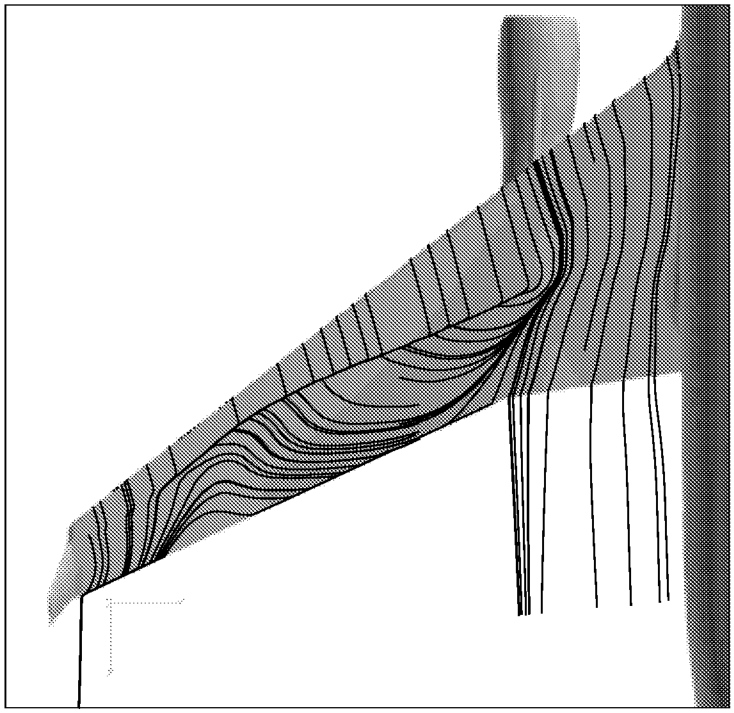

Figure 15: Wing upper surface streamlines, $\alpha = 5.2°$, CFL3D, SST.

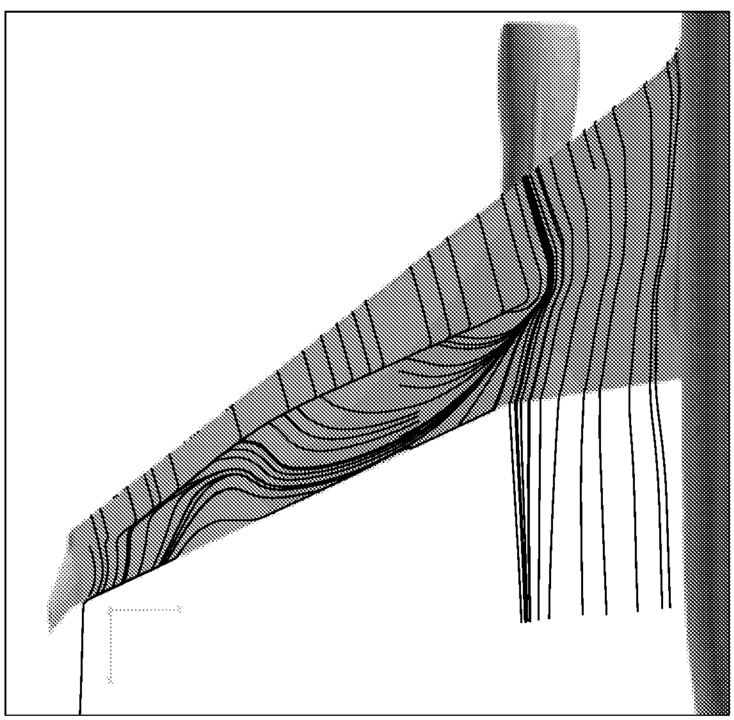

Figure 16: Wing upper surface streamlines, $\alpha = 5.2°$, CFL3D, EASM.

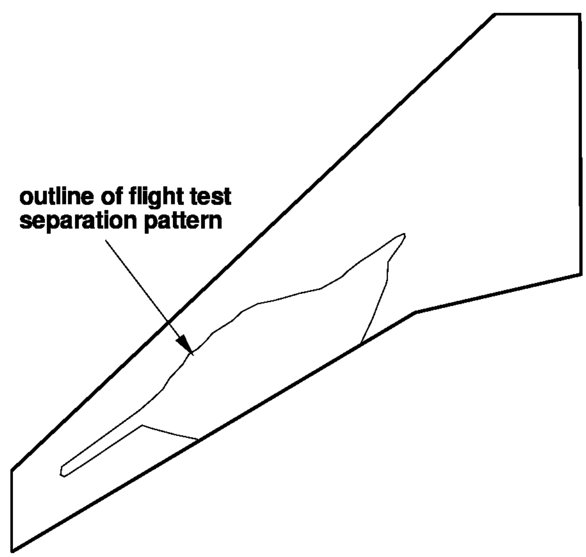

Figure 17: Schematic representation of flight test separation pattern on the wing upper surface, from Clark and Pelkman [8].

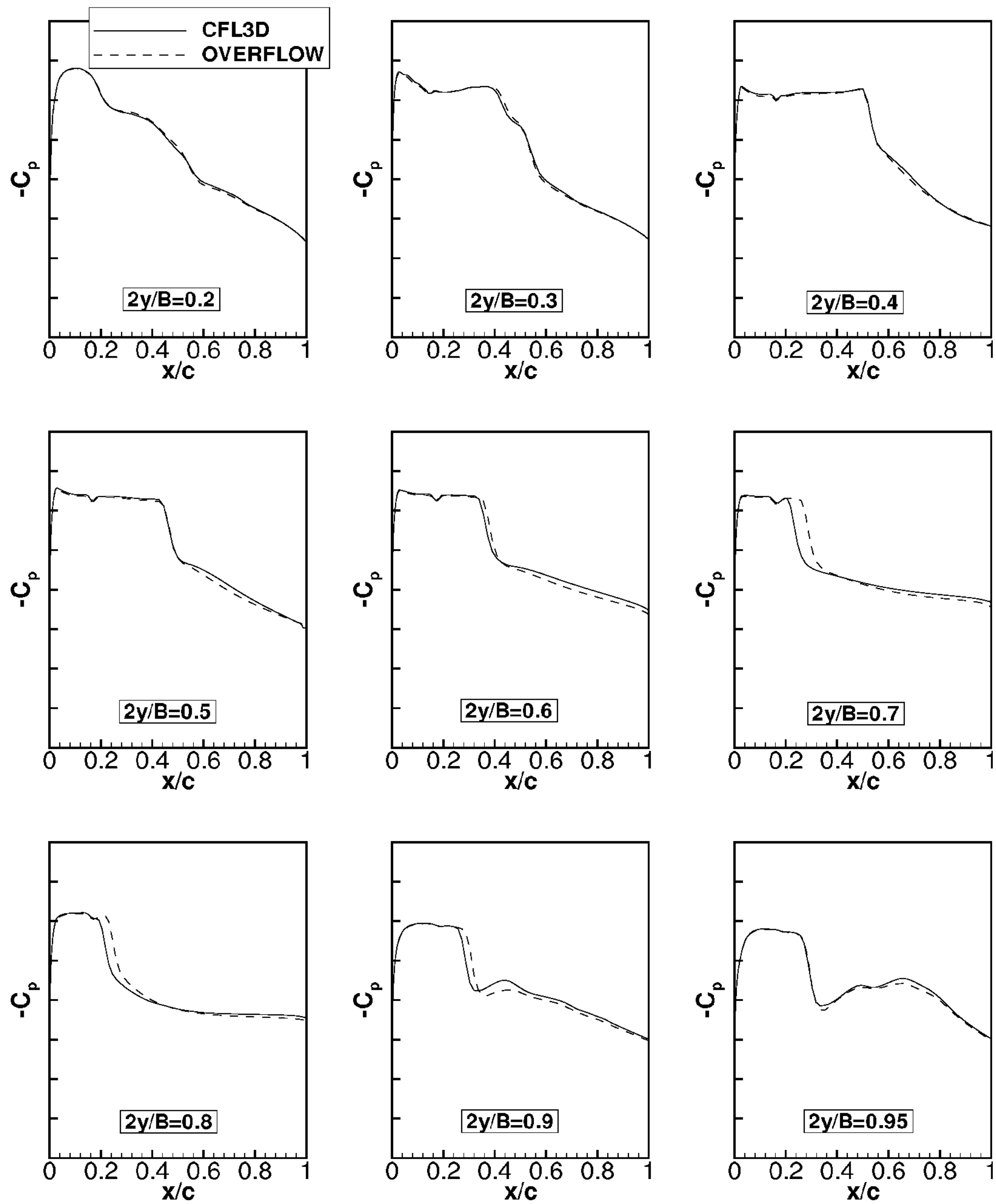

Figure 18: Effect of code on upper surface pressure coefficients, $\alpha = 5.2°$, SA.

4 CONCLUDING REMARKS

As a follow-on to an earlier study of CFD variation over a civil transport aircraft near buffet onset, a different aircraft configuration was studied. An overset grid was employed, with point distribution based on the lessons learned from the earlier study. The two codes OVERFLOW and CFL3D were used, and the effects of code, turbulence model, and trailing edge cap grid were studied. As in the earlier study, the turbulence model was found to have the largest effect, with a variation of 3.8% in lift at the buffet onset angle of attack. Drag and moment variation were 2.9% and 23.6%, respectively. The variations due to code and trailing edge cap grid were smaller than that due to turbulence model. Overall, the combined approximate error band in CFD due to code, turbulence model, and trailing edge treatment at the buffet onset angle of attack were: 4% in lift, 3% in drag, and 31% in moment. These numbers can be compared to those from the earlier buffet onset study (6% in lift, 7% in drag, and 16% in moment). The reason for the significantly larger percentage variation in the moment is due to the fact that the absolute moment values for the current configuration are approximately half those of the previous configuration. The absolute variations in moment levels are about the same. The current CFD results showed similar trends to flight test data, even well beyond buffet onset. However, the CFD results also exhibited a lift curve break not seen in the data. The reason for this difference is not known.

ACKNOWLEDGMENTS

The authors gratefully acknowledge the other members of the Buffet Onset Team - Steve Mysko and Dave Witkowski of Boeing, and Pieter Buning, Melissa Rivers, Dennis Allison, and Tom Gainer of NASA - for their helpful discussions during the work leading up to this study. Also, thanks go to Roger Clark and Deepak Om of Boeing, and Richard Wahls and James Thomas of NASA, for their guidance and support.

Table 1: Summary of computations performed at $M = 0.82$, $\mathrm{Re}_{\mathrm{MAC}} = 55$ million

Run	Grid	α, deg.	Code	Turbulence model
1	baseline 3.9	3.9	OVERFLOW	SA
2	baseline 4.3	4.3	OVERFLOW	SA
3	baseline 5.2	5.2	OVERFLOW	SA
4	baseline 5.2	6.0	OVERFLOW	SA
5	baseline 5.2	7.0	OVERFLOW	SA
6	baseline 5.2	8.0	OVERFLOW	SA
7	capped 3.9	3.9	OVERFLOW	SA
8	capped 4.3	4.3	OVERFLOW	SA
9	capped 5.2	5.2	OVERFLOW	SA
10	capped 5.2	6.0	OVERFLOW	SA
11	baseline 3.9	3.9	CFL3D	SA
12	baseline 4.3	4.3	CFL3D	SA
13	baseline 5.2	5.2	CFL3D	SA
14	baseline 3.9	3.9	CFL3D	SST
15	baseline 4.3	4.3	CFL3D	SST
16	baseline 5.2	5.2	CFL3D	SST
17	baseline 3.9	3.9	CFL3D	EASM
18	baseline 4.3	4.3	CFL3D	EASM
19	baseline 5.2	5.2	CFL3D	EASM
20	baseline 5.2	6.0	CFL3D	EASM

Table 2: Variation due to code (using SA model and baseline grids), in percent

α, deg	ΔC_L	ΔC_D	ΔC_M
3.9	0.3	0.4	7.6
4.3	1.1	0.7	12.0
5.2	1.3	1.6	10.4

Table 3: Variation due to turbulence model (using CFL3D and baseline grids), in percent

α, deg	ΔC_L	ΔC_D	ΔC_M
3.9	1.2	0.9	4.5
4.3	1.8	1.3	7.6
5.2	3.8	2.9	23.6

Table 4: Variation due to trailing edge cap grid (using OVERFLOW and SA model), in percent

α, deg	ΔC_L	ΔC_D	ΔC_M
3.9	0.4	0.1	2.4
4.3	0.3	0.3	1.9
5.2	0.9	1.5	5.9
6.0	1.5	2.4	10.2

References

[1] Rumsey, C. L., Allison, D. O., Biedron, R. T., Buning, P.G., Gainer, T. G., Morrison, J. H., Rivers, S. M., Mysko, S. J., Witkowski, D. P., "CFD Sensitivity Analysis of a Modern Civil Transport Near Buffet-Onset Conditions, NASA/TM-2001-211263, December 2001.

[2] Krist S. L., Biedron R. T., and Rumsey C. L., "CFL3D User's Manual (Version 5.0)", NASA TM-1998-208444, June 1998.

[3] Jespersen, D. C., Pulliam, T. H., and Buning, P. G., "Recent Enhancements to OVERFLOW," AIAA Paper 97-0644, Reno, NV, 1997.

[4] Suhs, N. E. and Tramel, R. W., "PEGSUS 4.0 User's Manual," Arnold Engineering Development Center Report AEDC-TR-91-8, November 1991.

[5] Spalart, P. R., and Allmaras, S. R., "A One-Equation Turbulence Model for Aerodynamic Flows," *La Recherche Aerospatiale*, No. 1, 1994, pp. 5–21.

[6] Menter, F. R., "Improved Two-Equation k-ω Turbulence Models for Aerodynamic Flows," NASA TM 103975, Oct. 1992.

[7] Rumsey, C. L., and Gatski, T. B., "Recent Turbulence Model Advances Applied to Multi-element Airfoil Computations," AIAA Paper 2000-4323, Denver, CO, 2000.

[8] Clark, R. W., and Pelkman, R. A., "High Reynolds Number Testing of Advanced Transport Aircraft Wings in the National Transonic Facility," AIAA Paper 2001-0910, Reno, NV, 2001.

REPORT DOCUMENTATION PAGE				Form Approved OMB No. 0704-0188

1. AGENCY USE ONLY (*Leave blank*)

2. REPORT DATE
February 2003

3. REPORT TYPE AND DATES COVERED
Technical Memorandum

4. TITLE AND SUBTITLE
CFD Variability for a Civil Tansport Aircraft Near Buffet-Onset Conditions

5. FUNDING NUMBERS
719-10-40-10

6. AUTHOR(S)
Christopher L. Rumsey, Joseph H. Morrison, and Robert T. Biedron

7. PERFORMING ORGANIZATION NAME(S) AND ADDRESS(ES)
NASA Langley Research Center
Hampton, VA 23681-2199

8. PERFORMING ORGANIZATION REPORT NUMBER
L-18256

9. SPONSORING/MONITORING AGENCY NAME(S) AND ADDRESS(ES)
National Aeronautics and Space Administration
Washington, DC 20546-0001

10. SPONSORING/MONITORING AGENCY REPORT NUMBER
NASA/TM-2003-212149

11. SUPPLEMENTARY NOTES

12a. DISTRIBUTION/AVAILABILITY STATEMENT
Unclassified-Unlimited
Subject Category 02 Distribution: Nonstandard
Availability: NASA CASI (301) 621-0390

12b. DISTRIBUTION CODE

13. ABSTRACT (*Maximum 200 words*)
A CFD sensitivity analysis is conducted for an aircraft at several conditions, including flow with substantial separation (buffet onset). The sensitivity is studied using two different Navier-Stokes computer codes, three different turbulence models, and two different grid treatments of the wing trailing edge. This effort is a follow-on to an earlier study of CFD variation over a different aircraft in buffet onset conditions. Similar to the earlier study, the turbulence model is found to have the largest effect, with a variation of 3.8% in lift at the buffet onset angle of attack. Drag and moment variation are 2.9% and 23.6%, respectively. The variations due to code and trailing edge cap grid are smaller than that due to turbulence model. Overall, the combined approximate error band in CFD due to code, turbulence model, and trailing edge treatment at the buffet onset angle of attack are: 4% in lift, 3% in drag, and 31% in moment. The CFD results show similar trends to flight test data, but also exhibit a lift curve break not seen in the data.

14. SUBJECT TERMS
Separated flow; Variability; Turbulence model

15. NUMBER OF PAGES
25

16. PRICE CODE

17. SECURITY CLASSIFICATION OF REPORT	18. SECURITY CLASSIFICATION OF THIS PAGE	19. SECURITY CLASSIFICATION OF ABSTRACT	20. LIMITATION OF ABSTRACT
Unclassified	Unclassified	Unclassified	UL